Lifetime, collisional-quenching, and j-mixing measurements of the metastable $3D$ levels of Ca^+

M. Knoop, M. Vedel, and F. Vedel*
Physique des Interactions Ioniques et Moléculaires (URA CNRS 773), Université de Provence, Case C21, F13397 Marseille Cedex 20, France
(Received 28 November 1994)

The metastable $3^2D_{3/2,5/2}$ doublet of Ca^+ ions stored in a Paul trap was investigated in the presence of different neutral gases, in the pressure range 10^{-9}–10^{-6} mbar. The natural lifetimes were determined to be $\tau(D_{3/2})=1111\pm46$ ms and $\tau(D_{5/2})=994\pm38$ ms, which agree very well with previous experiments. The estimation of the quenching rates of Ca^+-He [$\Gamma_{He}=(1.05\pm0.42)\times10^{-12}$ cm^3 s^{-1}], Ca^+-Ne [$\Gamma_{Ne}=(0.9\pm0.7)\times10^{-12}$ cm^3 s^{-1}], and Ca^+-N_2 [$\Gamma_{N_2}=(1.7\pm0.2)\times10^{-10}$ cm^3 s^{-1}] was carried out for collisions in the energy range 0.3–1.3 eV. In addition, rate constants for the mixing of the fine-structure states were measured in the presence of helium and nitrogen for the $j=3/2\rightarrow j=5/2$ case [γ_{35}(He)$=(2.24\pm0.10)\times10^{-10}$ cm^3 s^{-1} and $\gamma_{35}(N_2)=(2.8\pm0.3)\times10^{-9}$ cm^3 s^{-1}] and for the $j=5/2\rightarrow j=3/2$ case [γ_{53}(He)$=(1.2\pm0.7)\times10^{-10}$ cm^3 s^{-1} and $\gamma_{53}(N_2)=(1.26\pm0.10)\times10^{-9}$ cm^3 s^{-1}]. The measurements were carried out populating the metastable levels by direct laser excitation of the forbidden S-D transitions.

PACS number(s): 32.80.Pj, 32.50+d, 32.70.Cs

I. INTRODUCTION

The electrical quadrupole transition $4\,^2S_{1/2}$–$3\,^2D_{5/2}$ of Ca^+ at 729 nm offers an interesting possibility for a frequency standard in the optical domain, which could be achieved with the ion storage technique. The Q factor ($\nu/\Delta\nu$) of the proposed clock transition is higher than 10^{15} [1,2]. Under extreme conditions, the effect of the collisions with the particles of the background pressure is one of the main sources of the broadening of the clock transition and is difficult to eliminate [3]. On the other hand, the forbidden transitions of Ca II serve as calibration lines in astrophysics, where they are used to monitor densities and temperatures in stellar atmospheres [4,5]. For these applications, precise knowledge of lifetimes, quenching, and mixing rate constants is necessary. Theoretical computations of the metastable lifetimes with *ab initio* models using different approaches exist [6–8] and their comparison with experimental results is fundamental for improvement of the description needed for the numerical models.

The relevant energy levels of Ca II are shown in Fig. 1. The resonance lines H and K ($4\,^2S_{1/2}$–$4\,^2P_{1/2}$ and $4\,^2S_{1/2}$–$4\,^2P_{3/2}$) at 397 and 393 nm are very strong, $\tau(P_{1/2},P_{3/2})\approx7$ ns. The probabilities $A(4\,^2P$–$3\,^2D_j)$ of P-level relaxation toward the D states are high and the corresponding branching ratio $A(4\,^2P$–$4\,^2S_{1/2})/\Sigma_J A(4\,^2P$–$3\,^2D_J)$ has been measured to be 17.6 ± 1.0 [9].

The very few natural lifetime measurements of the $3\,^2D_{3/2}$ and $3\,^2D_{5/2}$ metastable states of Ca^+ that exist were all done with the ion storage technique. Two of these experiments were performed on an ion cloud at temperatures of 2000 K [10] and 8000 K [11]. The latest improvement of the method [11] leads to the following values $\tau(D_{3/2})=1113\pm45$ ms and $\tau(D_{5/2})=1054\pm61$ ms. Other experiments were performed with very few particles (2–4) [12] or a single laser-cooled ion [13]. The detection scheme for the latter experiment only allowed the determination of the $D_{5/2}$-level lifetime, found to be $\tau(D_{5/2})=1080\pm220$ ms, at an ionic temperature of 130 mK. The experiments discussed above concerned either a macroscopic [11] or a microscopic signal (quantum jumps) [13]. The population of the D levels was achieved by excitation of the S-P transitions followed by relaxation to the metastable states ("indirect population"). Observations were made on the S-P fluorescence either by probing the corresponding P-D transitions or by detecting quantum jumps in the case of a single ion.

The experiments presented here use another technique to investigate the $3\,^2D_j$ level by populating it by direct laser excitation of the corresponding $4\,^2S_{1/2}$–$3\,^2D_j$ transition. Compared to the indirect population mechanism, this method presents the advantage of avoiding parasitic population of the $3\,^2D_{3/2}$ level, which perturbs the measurements because of strong fine-structure mixing during the $3\,^2D_{5/2}$ study. In-

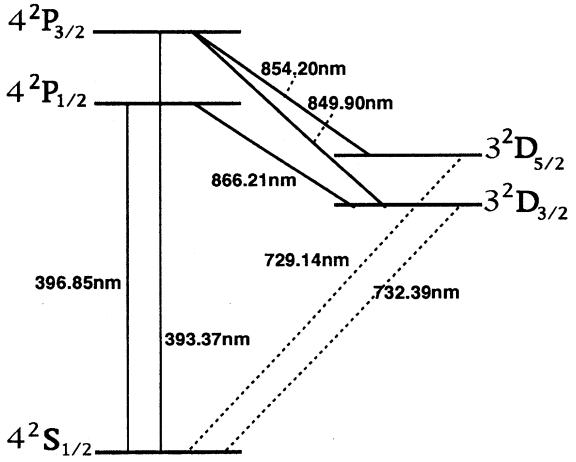

FIG. 1. Lower energy levels of Ca II.

*Author to whom correspondence should be addressed. FAX: +33 91 28 87 45. Electronic address: FERN@FRMRS11.U-3MRS.FR

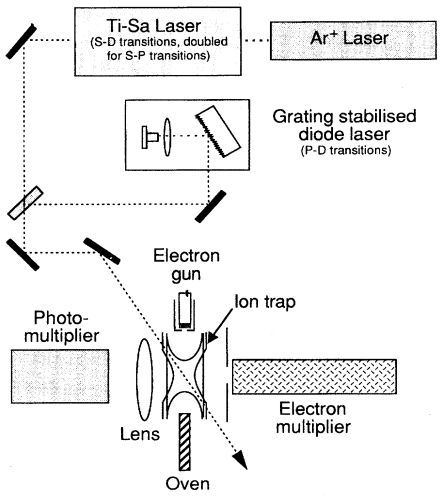

FIG. 2. Experimental setup.

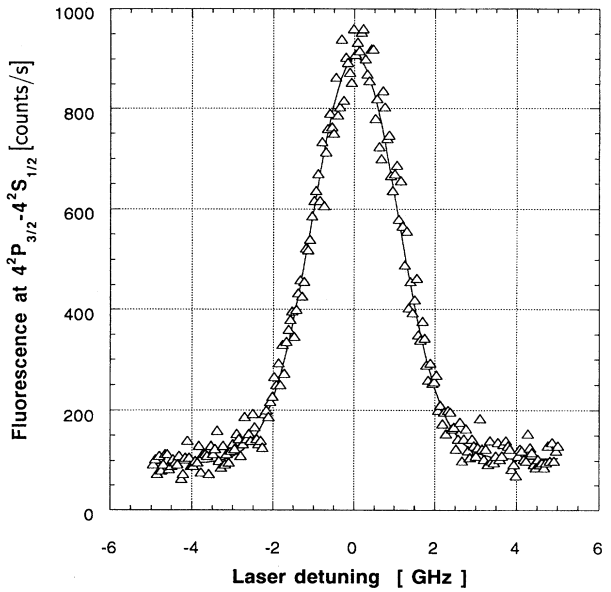

FIG. 3. Fluorescence of the $4P_{3/2}$-$4S_{1/2}$ transition during excitation of the $4S_{1/2}$-$3D_{5/2}$ transition and of the $3D_{5/2}$-$4P_{3/2}$ transition (P_{laser}=700 mW at 729 nm). The resonance profile is obtained by tuning the Ti-Sa laser, while the diode laser is kept at a fixed frequency.

deed, since collisions are almost always present, they prevent well-defined initial conditions. The latter could be obtained with an additional laser emptying the $3\,^2D_{3/2}$ level, but this would make the experiment even more complex.

This paper is organized as follows. In Sec. II we first describe the principle of the experiments. Then, in Sec. III A we present our results for the lifetime and the quenching rates measurements in the presence of neutral gases along with a discussion. Finally, in Sec. III B the fine-structure mixing is treated.

II. EXPERIMENTAL METHOD

The experimental setup is presented in Fig. 2. Further details can be found in Ref. [2]. Ca^+ ions are stored in a medium size, hyperbolic rf trap ($r_0=\sqrt{2}z_0=7.2$ mm). The ring of the trap is made from stainless steel and the end caps are formed from molybdenum mesh of high transmission (83%). The confinement radio frequency Ω is equal to $2\pi\times2$ MHz, the dc voltage V_{dc} varies between 0 and 10 V, and the ac voltage V_{ac} is around 420 V rms. Ultrahigh vacuum conditions are obtained with a turbomolecular pump (Balzers TPU060) and an ion pump (Méca2000 APID100) giving residual pressures lower than 10^{-9} mbar after 48 h of bakeout at 200 °C. Different neutral gases can be introduced into the vessel without contamination by impurities using a needle valve. Partial pressures are measured with a linear quadrupole mass spectrometer (Balzers QMG064), complemented by a Bayard-Alpert gauge. Calcium atoms are created by evaporation of metallic calcium from a small oven. They are ionized inside the trap with a pulsed electron gun and stored for times exceeding 1 h in a total pseudopotential well of 78 eV. The ion cloud has a temperature between 3000 and 15 000 K, depending on the pressure and the mass of the buffer gas [2].

The resonance radiation required for uv transitions is generated by a cw frequency-doubled titanium sapphire ring laser (Coherent 899-21), with a power up to 19 mW at 397 nm and a spectral width of 1 MHz. A laser diode, mounted in an external cavity, can be tuned in order to deliver the three D-P components (200 μW at 866 nm, spectral width less than 30 MHz). Finally, the S-D lines (729 and 732 nm) are available from the fundamental mode of the Ti-sapphire laser with power up to 1 W. The emitted photons are detected by a blue-peaked photomultiplier (Hamamatsu H4730), run in the photon-counting mode.

In the following, a discussion of the lifetime measurements will be presented. As mentioned above, we directly pump the investigated D level [2] instead of populating it by excitation of the S-P and relaxation of the P level, as in the previous Ca^+ experiments [10–13]. Figure 3 shows a typical fluorescence of the S-D transition that occurs during double-resonance excitation of the $4S_{1/2}$-$3D_{3/2}$ and $3D_{3/2}$-$4P_{1/2}$ transitions. The fluorescence of the $4S_{1/2}$-$4P_{1/2}$ transition is then detected, allowing the discrimination of the small ion signal from the large red background of scattered laser light by means of an interference filter. Experiments on the $4S_{1/2}$-$3D_{5/2}$ transition are carried out in a symmetric manner. The $D_{3/2}$ level ($D_{5/2}$, respectively) is populated by applying the titanium sapphire laser for approximately 1 s. After a variable time delay t_d, the D level is probed by the diode laser and the corresponding ultraviolet fluorescence is detected. We ascertained that the diode laser power, applied for 10 ms, was sufficiently high to empty the level completely. Between two successive times t_d and $t_d+\Delta t_d$ (where Δt_d varies between 5 and 200 ms, depending on the time constant of the temporal evolution investigated), the fluorescence signal diminishes proportionally to the D-state population. A sufficient precision can only be attained with the accumulation of data, where the number of accumulations is limited by the fact that the experimental conditions must be kept stable. In our experiments, the measurement of the full decay cycle was usually repeated 40 times. For each elementary decay

cycle, the relative ion loss is negligible.

Experiments have predicted the j mixing to be very fast in comparison to the quenching rate [14]. The temporal variation of the level populations is then governed by two deexcitation mechanisms: the depopulation process due to the finite lifetime of the atomic level and the quenching process. These are described by

$$\mathrm{Ca}^+(3D_j)\rightarrow \mathrm{Ca}^+(4S_{1/2})+h\nu, \quad \Gamma_{\mathrm{nat}}=\frac{1}{\tau_{\mathrm{nat}}}, \tag{1}$$

$$\mathrm{Ca}^+(3D_j)+A\rightarrow \mathrm{Ca}^+(4S_{1/2})+A+\Delta E, \quad \Gamma_Q, \tag{2}$$

where A is the neutral buffer gas (atom or molecule) present with density n_B. The quantities Γ_{nat} and Γ_Q are the corresponding rate constants. The excess energy ΔE appears as relative translational energy and also as change in rotational and vibrational degrees of freedom when A is a molecule. At a given buffer gas density n_B, we measure an effective lifetime τ_{meas}, given by

$$\frac{1}{\tau_{\mathrm{meas}}}=n_B\Gamma_Q+\frac{1}{\tau_{\mathrm{nat}}}. \tag{3}$$

The neutral gas must generally be considered as a mixture of the neutral atoms or molecules present, He, Ne, and N_2 (identified with an upper index i in the following). The rate constants differ for each species. Then

$$\frac{1}{\tau_{\mathrm{meas}}}=\sum_i n_B^i\Gamma_Q^i+\frac{1}{\tau_{\mathrm{nat}}}. \tag{4}$$

In order to determine the metastable lifetime in the absence of collisional deexcitation, we measured the effective lifetimes τ_{meas} for a wide range of different pressure values and compositions. The natural lifetime of the atomic level is then obtained by extrapolation to zero pressure. A multilinear fit allows the simultaneous determination of the unperturbed lifetime and the quenching rate for the neutral components.

The measurements of the collisional fine-structure mixing rates were obtained with a different method. Consider the case of the determination of the rate constant of the 5/2→3/2 mixing (j_{53}), where initially both fine-structure levels are empty. We populate the $D_{5/2}$ level by excitation of the $4S_{1/2}$-$3D_{5/2}$ transition. The neighboring $D_{3/2}$ state is filled exclusively by collisional population transfer from the $D_{5/2}$ level. A laser diode, tuned to the $3D_{3/2}$-$4P_{1/2}$ transition probes the population of the $3D_{3/2}$ level, which, as above, is monitored by the intensity of the fluorescence at 397 nm ($4P_{1/2}$-$4S_{1/2}$). The temporal evolution of the $D_{3/2}$ population is obtained by varying the delay t_{prob} between the end of the $D_{5/2}$ filling process and the beginning of $D_{3/2}$-level probing. For modeling the time dependence of $N_{5/2}(t)$, the following reactions have to be considered in addition to those Eqs. (1) and (2):

$$\mathrm{Ca}^+(3D_{3/2})+A\rightarrow \mathrm{Ca}^+(3D_{5/2})+A+\Delta E, \quad \gamma_{35} \tag{5}$$

and

$$\mathrm{Ca}^+(3D_{5/2})+A\rightarrow \mathrm{Ca}^+(3D_{3/2})+A+\Delta E, \quad \gamma_{53}. \tag{6}$$

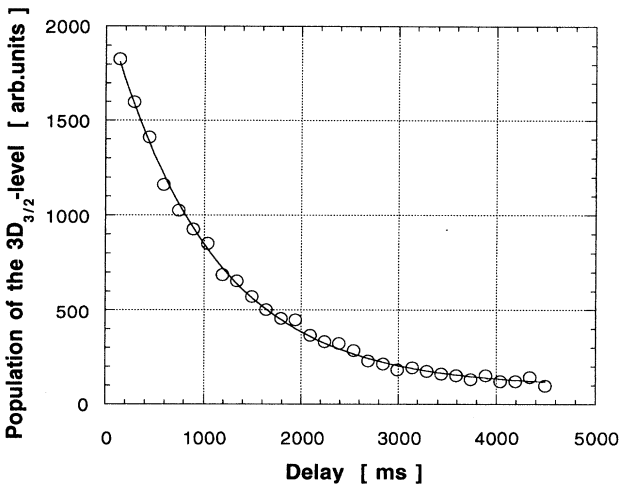

FIG. 4. Decrease of the $3D_{3/2}$-level population at a helium pressure of 1×10^{-7} mbar.

Assuming that the quenching rate constant Γ_Q is the same for both fine-structure levels and taking $N_{3/2}(t=0)=0$ and $N_{5/2}(t=0)=N_0$ as initial conditions, the analytical expression for the temporal evolution of the fine-structure levels is given by

$$N_{3/2}(t)=N_0\frac{\gamma_{53}}{\gamma_{53}+\gamma_{35}}[\exp(-\tfrac{1}{2}D_1t)-\exp(-\tfrac{1}{2}D_2t)], \tag{7}$$

$$N_{5/2}(t)=N_0\frac{1}{\gamma_{53}+\gamma_{35}}[\gamma_{35}\exp(-\tfrac{1}{2}D_1t)+\gamma_{53}\exp(-\tfrac{1}{2}D_2t)], \tag{8}$$

with $D_1=\Gamma_{\mathrm{nat}}+n_B\Gamma_Q$ and $D_2=\Gamma_{\mathrm{nat}}+n_B(\Gamma_Q+2\gamma_{35}+2\gamma_{53})$.

The measured effective mixing time constants τ_{53}, τ_{35} are a function of pressure and are related to the rate constants by

$$\frac{1}{\tau_{35}}=\sum_i n_B^i\gamma_{35}^i \quad \text{or} \quad \frac{1}{\tau_{53}}=\sum_i n_B^i\gamma_{53}^i. \tag{9}$$

In practice, in order to keep the $D_{3/2}$ level empty during population of the $D_{5/2}$ level [$N_{3/2}(t=0)=0$], a laser diode at 866 nm is applied simultaneously before starting the experiment.

III. RESULTS AND DISCUSSION

A. Quenching rates and the natural lifetime measurements

Both $3D$ levels were investigated in the presence of helium, neon, and molecular nitrogen. A typical ion population decrease is given in Fig. 4, which illustrates the $D_{3/2}$-level decay with helium at 1×10^{-7} mbar. The efficiency of the direct population method for the $D_{5/2}$-lifetime measurement can be seen in Fig. 5. Indeed, the effective lifetimes that we observed using the indirect population method are dispersed and far from the straight-line fitted with the data obtained with the direct method. The natural lifetimes, measured with

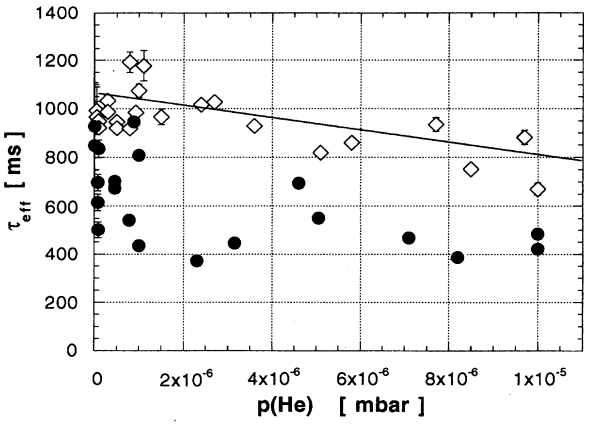

FIG. 5. Evidence of the influence of the initial conditions for the population of the $3D_{5/2}$ level. Measurements were made using indirect (●) and direct (Δ) population method.

the direct population method, were extrapolated by a multilinear fitting procedure with 80 points from a Stern-Vollmer plot as shown in Fig. 6. They were found to be $\tau(3D_{3/2})=1111\pm46$ ms and $\tau(3D_{5/2})=994\pm38$ ms. The uncertainty quoted is statistical only and at the 90% confidence level. As shown in Fig. 7, our values are in very good accord with $\tau(D_{3/2})=1113\pm45$ ms and $\tau(D_{5/2})=1054\pm61$ ms, which were measured recently at a residual pressure smaller than 7×10^{-10} mbar [11]. They can also be compared with the result obtained with a single laser-cooled ion [$\tau(D_{5/2})=1080\pm220$ ms] in Ref. [13], where the measurements were performed in the presence of hydrogen in the 10^{-10}–10^{-9} mbar range. Apparently, all experimental values measured so far are slightly inferior to the theoretical results [$\tau(D_{3/2})=1160$, 1271, and 1200 ms and $\tau(D_{5/2})=1140$, 1236, and 1160 ms [6–8]].

The quenching rates for the buffer gases used are deduced from the data represented in Fig. 6 and are

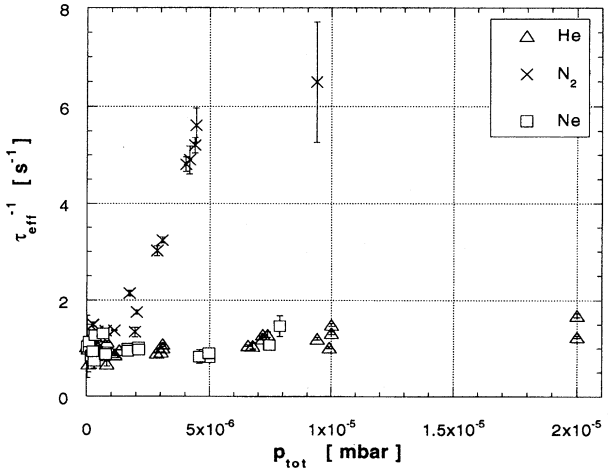

FIG. 6. Stern-Vollmer plot for quenching of the $3\,^2D_{3/2}$ level.

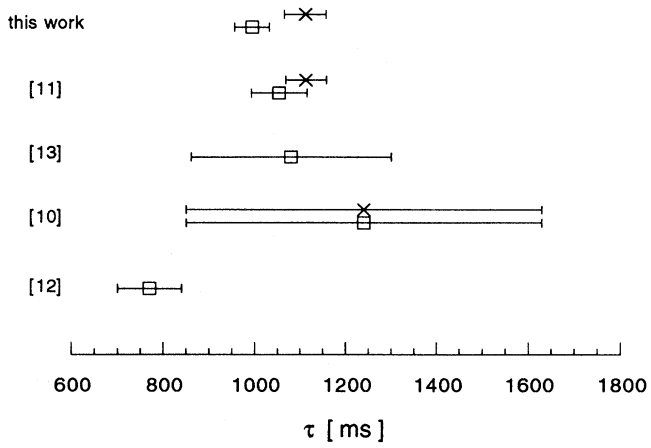

FIG. 7. Presentation of the experimentally determined metastable lifetimes (□, $D_{5/2}$; ×, $D_{3/2}$).

$$\Gamma_Q(\mathrm{He})=(1.05\pm0.42)\times10^{-12}\ \mathrm{cm^3\ s^{-1}},$$

$$\Gamma_Q(\mathrm{Ne})=(0.9\pm0.7)\times10^{-12}\ \mathrm{cm^3\ s^{-1}},$$

$$\Gamma_Q(\mathrm{N_2})=(1.7\pm0.2)\times10^{-10}\ \mathrm{cm^3\ s^{-1}}.$$

The ion energy varies in our experiment from 0.3 to 1.3 eV. We assume that the quenching rate constants do not depend strongly on the energy of the collision, which varies with the pressure conditions because of the collisional cooling effect. The uncertainties in our data originate mostly in the error in the absolute pressure measurements (almost 30%). The contribution of the residual components is always less than 0.5%.

We can roughly estimate the corresponding cross sections from the approximation $\Gamma_Q=\langle\sigma v\rangle=\langle\sigma\rangle\langle v\rangle$, where $\langle v\rangle$ is the average velocity in the center of mass, given by $\langle v\rangle=(8k_BT/\pi\mu)^{1/2}$, μ is the reduced mass of the Ca^+–buffer-gas system, and T is the temperature in the center-of-mass system. In fact, for the determination of T, the assumption is made that the temperature of the buffer gas (~300 K) is negligible compared to the ion temperature, which is usually defined for trapped ion clouds. This leads to the quenching cross sections σ_Q at 10 000 K presented in Table I.

The measured rate constants can be compared with the Langevin capture rate constant k_L given by

$$k_L=\frac{q}{2\varepsilon_0}\left(\frac{\alpha}{\mu}\right)^{1/2}, \tag{10}$$

where q is the electric charge of the ion and α its polarizability [15]. The ratios between the rate constants of quenching and the corresponding k_L are very small and of the same order of magnitude for rare-gas–Ca^+ systems. This ratio is 100 times larger for Ca^+-N_2, which shows the major role played by the deexcitation to the ground state in the collision process, when a molecular gas is involved.

Comparable values for $\Gamma_Q(\mathrm{He})$ and $\Gamma_Q(\mathrm{N_2})$ have been measured by Gudjons [$\Gamma_Q(\mathrm{He})=(8\pm1.85)\times10^{-13}$ cm^3 s^{-1} and $\Gamma_Q(\mathrm{N_2})=(1.1\pm1.78)\pm10^{-10}$ cm^3 s^{-1}] [16]. On the

TABLE I. Quenching rate constants and cross sections of $Ca^+(3D)$ due to collisions with different buffer gases.

Gas	$\Gamma_Q[cm^3\ s^{-1}]$	$\sigma_Q[Å^2]$ at 10^4 K	$k_L[cm^3\ s^{-1}]$	$\frac{\Gamma_Q}{k_L}$
He	$(1.05\pm 0.40)\times 10^{-12}$	0.020 ± 0.009	5.6×10^{-10}	0.0019
Ne	$(0.9\pm 0.7)\times 10^{-12}$	0.034 ± 0.026	4×10^{-10}	0.0022
N_2	$(1.7\pm 0.2)\times 10^{-10}$	7.10 ± 0.85	7.5×10^{-10}	0.23

other hand, the rate constants for collisions with N_2 do not seem to depend strongly on the ion species since for Ba^+-N_2 they were found to be $(4.3\pm 0.3)\times 10^{-11}$ $cm^3\ s^{-1}$ [17] and $(2.2\pm 0.3)\times 10^{-10}$ $cm^3\ s^{-1}$ [18] and for Yb^+-N_2, $(1.78\pm 0.19)\times 10^{-10}$ $cm^3\ s^{-1}$ [19]. To our knowledge, the quenching rate constant for the metastable $3D$ levels of Ca^+ during collisions with neon has never been measured before.

B. j-mixing rates

The mixing rate constants were measured for the case of helium and nitrogen. A typical curve of the temporal evolution of the population of the level investigated is shown in Fig. 8 ($D_{3/2}$ level at a helium pressure of 3×10^{-7} mbar). The j-mixing rates are determined by application of χ^2 minimization using Eq. (7). From the corresponding Stern-Vollmer plot (shown in Fig. 9), we deduce the mixing rates for He:

$$\gamma_{35}(\mathrm{He})=(2.24\pm 0.1)\times 10^{-10}\ \ cm^3\ s^{-1},$$

$$\gamma_{53}(\mathrm{He})=(1.20\pm 0.7)\times 10^{-10}\ \ cm^3\ s^{-1}.$$

In the presence of molecular nitrogen, we find

$$\gamma_{35}(N_2)=(2.8\pm 0.3)\times 10^{-9}\ \ cm^3\ s^{-1},$$

$$\gamma_{53}(N_2)=(1.26\pm 0.1)\times 10^{-9}\ \ cm^3\ s^{-1}.$$

Because of the small energy difference between the fine-structure levels (7.4 meV), negligible in comparison to the translation energy, we can use the principle of detailed balancing to determine the relation between γ_{35} and γ_{53}:

$$\frac{\gamma_{35}}{\gamma_{53}}=\frac{3}{2}\exp\left(-\frac{\Delta E_{3/2-5/2}}{k_B T}\right). \tag{11}$$

This relation gives the estimation

$$\gamma_{35}\cong 1.5\gamma_{53}, \tag{12}$$

which is almost that of the experimental results (within the given error limits)

$$\frac{\gamma_{35}(\mathrm{He})}{\gamma_{53}(\mathrm{He})}=1.8\pm 0.9,\quad \frac{\gamma_{35}(N_2)}{\gamma_{53}(N_2)}=2.2\pm 0.4.$$

Measurements at equilibrium allow the confirmation of the j-mixing rate constants values. At different pressure values we compare the fluorescence signals in the ultraviolet ($S_{1/2}$-$P_{1/2}$ and $S_{1/2}$-$P_{3/2}$) if the $D_{3/2}$ level is directly laser excited (then probed at the $D_{3/2}$-$P_{1/2}$ transition) while the other D level is exclusively populated by collisional mixing and probed at the $D_{5/2}$-$P_{3/2}$ transition (sensitized fluorescence technique [20,21]). This study was carried out using helium as a buffer gas.

At around 10^{-6} mbar, the difference of these fluorescence signals ($I_{3/L}$-$I_{5/2}$) is close to zero because the $3D$ levels are almost completely mixed. At lower pressures, mixing collisions become less important and the fluorescence signals of

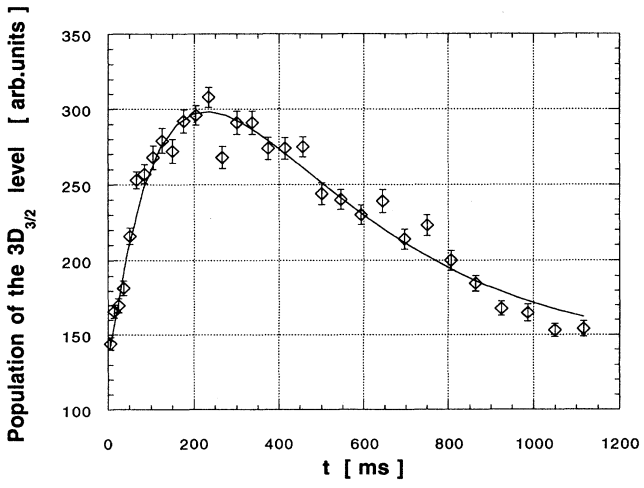

FIG. 8. Temporal evolution of the population of the $3D_{3/2}$ level during fine-structure mixing at $p(\mathrm{He})=3\times 10^{-7}$ mbar.

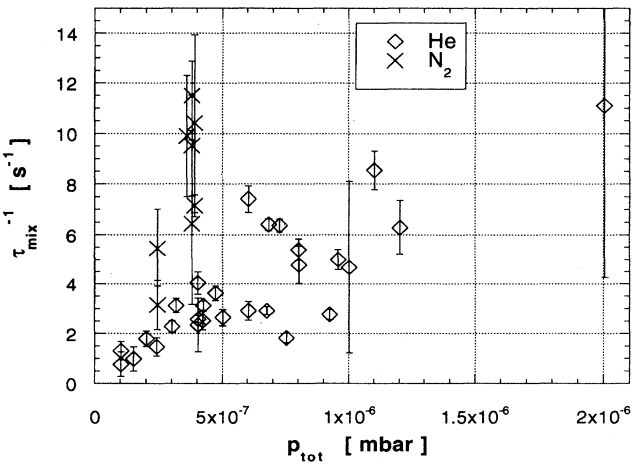

FIG. 9. Stern-Vollmer plot for $3D_{3/2}\rightarrow 3D_{5/2}$ mixing.

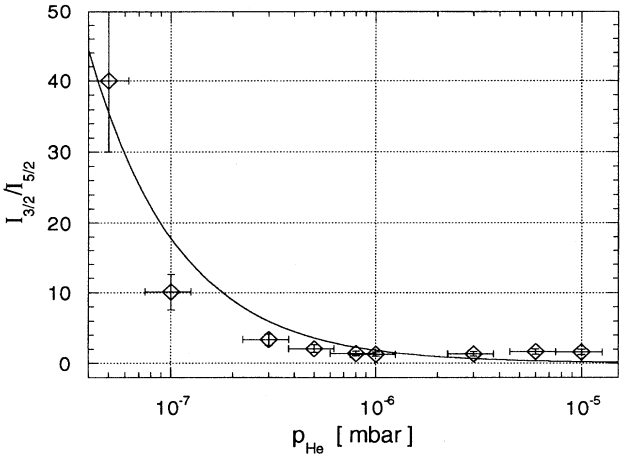

FIG. 10. Intensity ratio of the two signals resulting from the measurements of sensitized fluorescence versus buffer gas pressure.

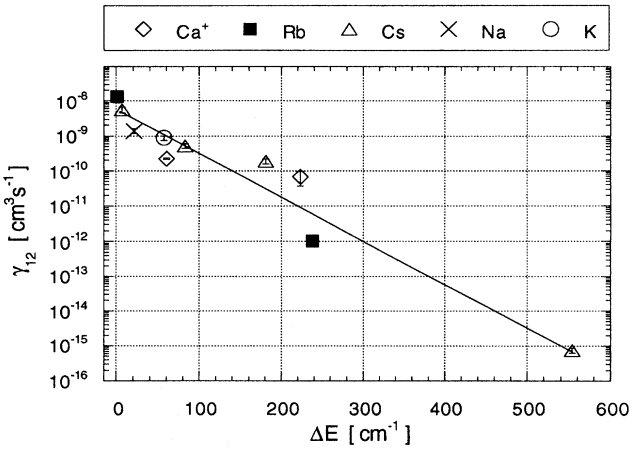

FIG. 11. j-mixing rate constants for different alkaline atoms and alkaline-earth ions in the presence of helium, as a function of the energy difference of the two levels involved, from Refs. [21–26]; the considered atomic species are given in the reference list.

the collisionally populated level vanish. For higher pressures, the small effective lifetimes due to quenching collisions prevent the system from attaining the equilibrium state [2].

Taking into account Eq. (12), the ratio of the fluorescence intensities $I_{3/2}/I_{5/2}$ is, at small optical densities, given by

$$\frac{I_{3/2}}{I_{5/2}} = \frac{\Gamma_{\text{nat}} + \Gamma_Q n_B}{2\gamma_{35} n_B} + \text{const.} \tag{13}$$

From our measurements (Fig. 10) and Eq. (13) we obtain a rate constant for the mixing from $D_{3/2}$ to $D_{5/2}$:

$$\gamma_{35}(\text{He}) = (2.6 \pm 0.9) \times 10^{-10} \text{ cm}^3 \text{ s}^{-1}.$$

In spite of the errors (the main uncertainty arises from the small number of points), this estimate agrees very well with the results presented above.

Our measurements exhibit a quantitative difference between the velocities of the quenching and the mixing processes. Quenching of the metastable states takes place much slower than mixing of fine-structure levels. In fact, nonadiabatic transitions have a small probability if the splitting between the adiabatic states is important. Due to the comparatively weak spin-orbit coupling, intermultiplet transitions are therefore favored during collision processes. As for quenching, a molecular buffer gas gives rise to mixing rate constants that are much higher than for the rare-gas case. In fact, during collisions between an atom and a diatomic molecule, the presence of a greater number of possible configurations increases the probability for nonadiabatic crossing between terms of the same symmetry. We can also estimate the strength of the interaction by comparing our data with the Langevin rate constant. Here the ratio k_L/γ_{ij} is equal to 0.1 for helium and is of the order of 10 for N_2, which indicates the long-range interaction efficiency in the Ca^+-N_2 system.

The measurements we made with Ca^+ and helium as a buffer gas can be compared with other j-mixing rate constants (Fig. 11) that have been obtained for collisions between helium and different alkaline atoms [21–26]. We recall that the energy-level structures of alkaline atoms and of alkaline-earth ions are very similar; therefore, in a first approximation these species can be compared quite well. We observe that the j-mixing rates can be roughly described by the semiclassical approach of the theory of Landau-Zener [27,28], which establishes that the transition probability between two atomic levels during a collision is inversely proportional to an exponential function of the energy of the transition. We can also show that the strength of the transition has no apparent influence on the mixing rate. Here optical selection rules seem not to be valid for collisional deexcitation processes. Compared to the measurements that have been made with alkaline atoms ($p_{\text{buffer gas}} = 10^{-1}$–$10^2$ mbar), our experiments have been performed in a considerably lower pressure regime. The time constants for the mixing of two metastable fine-structure levels are then quite slow, which allows the resolution of the j-mixing dynamics. This method gives higher precision results than those attainable by the method of sensitized fluorescence.

IV. CONCLUSION

In this paper we have presented measurements concerning the dynamics of the metastable levels of Ca^+ in the presence of buffer-gas collisions. We have determined values for the natural lifetimes, which are in very good agreement (magnitude and precision) with other experiments. They confirm the more recent data of the natural lifetimes of the $3D$ levels of Ca II. We have also measured rate constants for quenching and mixing in the presence of helium, neon, and nitrogen. Quenching and j mixing are common phenomena, particularly in astrophysics, and there exists only partial experimental data, which are rarely consolidated by different measurements. The data given in this work complete previous experiments by increasing the precision or by giving alternative collision partners such as, for example, $\Gamma(Ca^+\text{-Ne})$ for quenching and $\gamma(Ca^+\text{-He})$ and $\gamma(Ca^+\text{-}N_2)$ for mixing. Mixing and quenching rate constants for different ion–neutral-atom pairs can be estimated by application of the Landau-Zener model. However, a realistic application of this model

requires more detailed descriptions that take into account the relative importance of the molecular and the spin-orbit interactions. Knowledge of the adiabatic potentials (the relative positions of the involved states, the repulsivity, and the strength of attraction) is essential. Due to the presence of the additional Coulomb interaction and the relative complexity of the D state leading to Δ molcular states, approximate potentials are not precise enough. Multireference configuration-interaction methods are now planned for the determination of Ca^+–rare-gas intermolecular potentials.

ACKNOWLEDGMENTS

This work was supported by Direction Générale des Recherches et des Etudes Techniques. M.K. is grateful to the EC (Human Capital and Mobility Program) for financial support.

[1] G. Werth, in *Applied Laser Spectroscopy*, Proceedings of the Summer School, San Miniato, 1989, edited by W. Demtröder, and M. Inguscio (Springer, Berlin, 1989).

[2] M. Knoop, M. Vedel, and F. Vedel, J. Phys. (France) II **4**, 1639 (1994).

[3] D. J. Wineland, J. C. Bergquist, J. J. Bollinger, W. M. Itano, F. L. Moore, J. M. Gilligan, M. G. Raizen, D. J. Heinzen, C. S. Weimer, and C. H. Manney, in *Laser Manipulation of Atoms and Ions*, Proceedings of the International School of Physics "Enrico Fermi," Course CXVIII, Varenna, 1992, edited by E. Arimondo, W. D. Phillips, and F. Strumia (North-Holland, Amsterdam, 1992).

[4] L. M. Hobbs, A. M. Lagrange-Henri, R. Ferlet, A. Vidal-Majar, and D. E. Welty, Astrophys. J **334**, L41 (1988).

[5] C. Zeippen, Astron. Astrophys. **229**, 248 (1990).

[6] C. Guet and W. R. Johnson, Phys. Rev. A **44**, 1531 (1991).

[7] N. Vaeck, M. Godefroid, and C. Froese Fischer, Phys. Rev. A **46**, 3704 (1992).

[8] T. Brage, C. Froese Fischer, N. Vaeck, M. Godefroid, and A. Hibbert, Phys. Scr. **48**, 533 (1993).

[9] A. Gallagher, Phys. Rev. **157**, 24 (1967).

[10] F. Arbes, T. Gudjons, F. Kurth, G. Werth, F. Marin, and M. Inguscio, Z. Phys. D **25**, 295 (1993).

[11] F. Arbes, M. Benzing, T. Gudjons, F. Kurth, and G. Werth, Z. Phys. D **29**, 159 (1994).

[12] S. Urabe, M. Watanabe, H. Imajo, and K. Hayasaka, Opt. Lett. **17**, 1140 (1992).

[13] S. Urabe, K. Hayasaka, M. Watanabe, H. Imajo, R. Ohmukai, and R. Hayashi, Appl. Phys. B **57**, 367 (1993).

[14] D. A. Miller, L. You, J. Cooper, and A. Gallagher, Phys. Rev. A **46**, 1303 (1992).

[15] E. W. McDaniel, *Collision Phenomena in Ionized Gases* (Wiley, New York, 1964).

[16] T. Gudjons, Diplomarbeit, University of Mainz, 1993 (unpublished).

[17] A. Madej and D. J. Sankey, Phys. Rev. A **41**, 2621 (1990).

[18] A. Hermanni and G. Werth, Z. Phys. D **11**, 301 (1989).

[19] C. Gerz, J. Roths, F. Vedel, and G. Werth, Z. Phys. D **8**, 235 (1988).

[20] A. C. G. Mitchell and M. W. Zemansky, *Resonance Radiation and Excited Atoms* (Cambridge University Press, Cambridge, 1961).

[21] M. Pimbert, J. Phys. (Paris) **33**, 331 (1972); j-mixing rate constants for Cs($8P$)-He.

[22] J. Brust, M. Movre, and K. Niemax, Z. Phys. D **27**, 243 (1993); j-mixing rate constants for Ca^+($4P$)-He.

[23] T. R. Mallory, W. Kedzierski, J. B. Atkinson, and L. Krause, Phys. Rev. A **38**, 5917 (1988); j-mixing rate constants for Rb($9D$)-He.

[24] M. Lukaszewkski and I. Jackowska, J. Phys. B **21**, L659 (1988); j-mixing rate constants for Cs($9D$)-He.

[25] L. Krause, Appl. Opt. **5**, 1375 (1966); j-mixing rate constants for Na($3P$)-He, K($4P$)-He, Rb($5P$)-He, and Cs($6P$)-He.

[26] J. Cuvellier, P. R. Fournier, F. Gounand, and J. Berlande, C. R. Acad. Sci. Paris B **276**, 855 (1973); j-mixing rate constants for Cs($7P$)-He.

[27] N. F. Mott and H. S. W. Massey, *The Theory of Atomic Collisions* (Clarendon, Oxford, 1965).

[28] E. E. Nikitin, *Theory of Elementary Atomic and Molecular Processes in Gases* (Clarendon, Oxford, 1974).

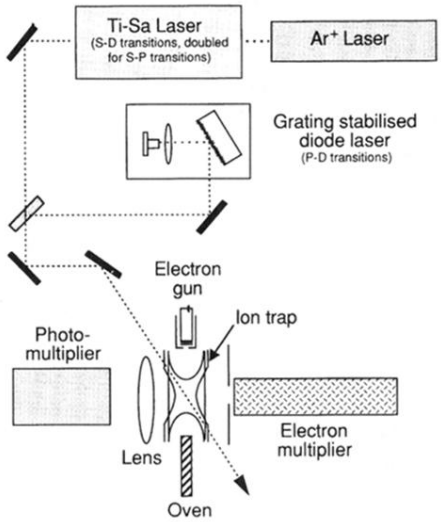

FIG. 2. Experimental setup.